

Wave propagation in the presence of empty cracks in elastic slabs – TBEM and MFS Formulations

A. Tadeu¹, L. Godinho¹, J. António¹ and P. Amado Mendes¹

Summary

This paper evaluates the 3D wave propagation in an elastic slab containing cracks whose geometry does not change along the direction parallel to the formation surfaces. Two different formulations are used and compared: the Traction Boundary Element Method (TBEM) and the Method of Fundamental Solutions (MFS). Both approaches are developed in the frequency domain and surmount the thin-body difficulty posed by the classical Boundary Element Method (BEM).

The TBEM models the crack as a single line. The resulting hypersingular integrals are evaluated analytically. For the MFS, the solution is approximated in terms of a linear combination of fundamental solutions, generated by a set of virtual sources that simulate the scattered field produced by the crack. A domain decomposition technique avoids the use of any enriched function to model displacement jumps across the crack.

Introduction

The use of the TBEM solution overcomes the difficulties posed by the classical BEM when solving very thin bodies or cracks [1]. In the case of a dimensionless empty crack, the problem can be solved using only a single line of boundary elements loaded with dipole loads [2]. The resulting hypersingular integrals can be computed analytically by defining the dynamic equilibrium of semi-cylinders above the boundary elements discretizing the crack [3].

This paper addresses the problem of wave propagation in the vicinity of 2D empty cracks, placed in a free elastic slab and subject to a point blast load. The use of appropriate Green's functions renders the discretization of the slab surfaces unnecessary. However, this model leads to high computational costs.

To mitigate some of these difficulties, the MFS can be an alternative option. The solution is obtained by a linear combination of fundamental solutions (Green's functions), generated by a set of virtual sources which, in the context of the present problem, can simulate the scattered field produced by the empty crack, using a domain decomposition technique. To avoid singularities, the fictitious sources are not placed along the crack boundary. The use of fundamental solutions allows the final solution to verify the unbounded boundary conditions automatically.

Some authors have proposed the use of enrichment functions to model torsional problems, including cracks [4]. Alternatively, a domain decomposition technique

¹Department of Civil Engineering, Faculty of Sciences and Technology, University of Coimbra, Portugal

can be used, adopting two elastic domains defined by a closed line that incorporates the crack surface. Along the crack, null stresses are imposed, while along the remaining part of that closed line, i.e. the virtual interface, continuity of stresses and displacements is prescribed.

Next, the problem, the TBEM and MFS formulations are established. The performance of the proposed models is compared. Finally, the applicability of the MFS is illustrated by computing (in the time domain) the scattered wavefield produced by an empty S-shaped crack embedded in an elastic slab.

Problem definition

An empty 2D crack aligned along the z axis is buried in a solid layer with thickness h (density ρ , shear wave velocity β and dilatational wave velocity α). This system is excited by a harmonic cylindrical line source at (x_s, y_s) , oscillating with angular frequency ω and spatially varying along the z direction. The direct incident field is given by a dilatational potential $\hat{\phi}$,

$$\hat{\phi}_{inc}(\omega, x, y, k_z) = \frac{-iA}{2} H_0 \left(k_\alpha \sqrt{(x-x_s)^2 + (y-y_s)^2} \right), \quad (1)$$

where A is the amplitude, $H_n(\cdot)$ are second Hankel functions of order n , $k_\alpha = \sqrt{\omega^2/\alpha^2 - k_z^2}$ with $\text{Im}(k_\alpha) < 0$, k_z is the axial wavenumber and $i = \sqrt{-1}$.

Traction Boundary Element Formulation (TBEM)

The TBEM formulation is expressed by the following equation:

$$a u_i(\mathbf{x}_0, \omega) = - \int_S u_j(\mathbf{x}, \omega) \bar{H}_{ij}(\mathbf{x}, \mathbf{n}_n, \mathbf{x}_0, \omega) ds + \bar{u}_i^{inc}(\mathbf{x}_s, \mathbf{x}_0, \mathbf{n}_n, \omega). \quad (2)$$

In the equation, $i, j = 1, 2$ correspond to the normal and tangential directions relative to the inclusion's surface, respectively, while $i, j = 3$ correspond to the z direction. $u_j(\mathbf{x}, \omega)$ corresponds to displacements in direction j at \mathbf{x} . The coefficient a is null for piecewise straight boundary elements [1]. $\bar{H}_{ij}(\mathbf{x}, \mathbf{n}_n, \mathbf{x}_0, \omega)$ is obtained after applying the traction operator to $H_{ij}(\mathbf{x}, \mathbf{n}_n, \mathbf{x}_0, \omega)$, which defines the tractions in direction j at \mathbf{x} (on the boundary S), due to a unit point force in the direction i at \mathbf{x}_0 (a collocation point). $\mathbf{n}_n = (\cos \theta_n, \sin \theta_n)$ defines the unit outward normal relative to the boundary element, at \mathbf{x} . Performing the equilibrium of stresses, the following equations can be written along x, y and z , caused by loads also applied along the same x, y and z directions:

$$\begin{aligned} \bar{H}_{xr} &= 2\mu \left[\frac{\alpha^2}{2\beta^2} \frac{\partial H_{xr}}{\partial x} + \left(\frac{\alpha^2}{2\beta^2} - 1 \right) \left(\frac{\partial H_{yr}}{\partial y} + \frac{\partial H_{zr}}{\partial z} \right) \right] \cos \theta_0 + \mu \left[\frac{\partial H_{yr}}{\partial x} + \frac{\partial H_{xr}}{\partial y} \right] \sin \theta_0 \\ \bar{H}_{yr} &= 2\mu \left[\left(\frac{\alpha^2}{2\beta^2} - 1 \right) \left(\frac{\partial H_{xr}}{\partial x} + \frac{\partial H_{zr}}{\partial z} \right) + \frac{\alpha^2}{2\beta^2} \frac{\partial H_{yr}}{\partial y} \right] \sin \theta_0 + \mu \left[\frac{\partial H_{yr}}{\partial x} + \frac{\partial H_{xr}}{\partial y} \right] \cos \theta_0 \end{aligned} \quad (3)$$

$$\bar{H}_{zr} = \mu \left[\frac{\partial H_{xr}}{\partial z} + \frac{\partial H_{zr}}{\partial x} \right] \cos \theta_0 + \mu \left[\frac{\partial H_{yr}}{\partial z} + \frac{\partial H_{zr}}{\partial y} \right] \sin \theta_0,$$

where $\mathbf{n}_0 = (\cos \theta_0, \sin \theta_0)$ defines the unit outward normal at \mathbf{x}_0 , $\bar{H}_{tr} = \bar{H}_{tr}(\mathbf{x}, \mathbf{n}_n, \mathbf{x}_0, \omega)$, $H_{tr} = H_{tr}(\mathbf{x}, \mathbf{n}_n, \mathbf{x}_0, \omega)$, with $r, t = x, y, z$ and $\mu = \rho \beta^2$. The tractions $H_{tr}(\mathbf{x}, \mathbf{n}_n, \mathbf{x}_0, \omega)$ are obtained by derivatives of the Green's functions for the elastic slab [6]. Similarly, the incident field components in terms of stresses ($\bar{u}_r^{inc} = \bar{u}_r^{inc}(\mathbf{x}_s, \mathbf{x}_0, \mathbf{n}_n, \omega)$) can also be evaluated by means of derivatives of the displacement incident field at \mathbf{x}_0 , generated by a source placed in that medium at \mathbf{x}_s ($u_r^{inc} = u_r^{inc}(\mathbf{x}_s, \mathbf{x}_0, \omega)$).

After the discretization of the boundary, the resulting hypersingular integrals can be evaluated analytically [3]. After the nodal displacement unknowns have been obtained, the response at any point inside the domain, \mathbf{x}_{rec} , can be computed by solving the classical boundary integral equation.

Meshless Solution - The MFS Formulation

The solution is approximated in terms of a linear combination of fundamental solutions, generated by a set of virtual sources that simulate the scattered field generated by the inclusion (see Figure 1). In order to avoid singularities, these fictitious sources are placed outside the physical domain of the stated problem [7].

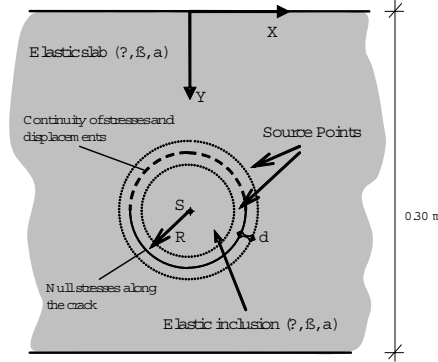


Figure 1: Schematic representation of the MFS model.

Two sets of NS virtual loads are distributed along the inclusion interface at distances δ from that boundary towards the interior and exterior of the inclusion. For each position, the loads are applied in the x , y , and z directions. Sources inside the inclusion have unknown amplitudes $a_{rn}^{(1)}$, while those placed outside the inclusion have unknown amplitudes $a_{rn}^{(2)}$. n is the subscript that denotes the load order number, and r the direction in which the load is applied. In each medium, the reflected displacements are given by

$$u_t^{(m)}(\mathbf{x}, \omega) = \sum_{n=1}^{NS} \left[\sum_{r=1}^3 \left[a_{rn}^{(m)} G_{rt}^{(m)}(\mathbf{x}, \mathbf{x}_n, \omega) \right] \right] \quad (4)$$

where $G_{rt}^{(m)}(\mathbf{x}, \mathbf{x}_n, \omega)$ is the fundamental solution which represents the displacement at point $\mathbf{x} = (x, y)$, in medium m (1, 2), in the direction t generated by a load acting along r at position $\mathbf{x}_n = (x_n, y_n)$.

To determine the unknown amplitude loads, it is necessary to impose the boundary conditions of continuity of tangential and normal displacements and stresses along the virtual boundary not coinciding with the crack and null stresses along the crack surface. After solving the resulting system of equations, the displacements in the solid domains can be determined.

Performance of the MFS algorithm

A C-shaped empty crack, embedded in a solid free layer, illustrated above in Figure 1, is used to verify the MFS's performance. The properties of the slab's elastic material are $\alpha = 2696.5$ m/s, $\beta = 1451.7$ m/s and $\rho = 2140$ kg/m³. The crack, with a radius of $R = 0.05$ m, is centered at (0m, 0.175 m) and the spatially sinusoidal harmonic line load is placed at S (0m, 0.175 m).

The frequency of $f = 10000$ Hz, with $k_z = 25$ rad/m, is selected to illustrate the main conclusions. The results are evaluated over a grid of receivers placed around the crack. The crack is discretized using 200 boundary elements to ensure the accurate response of the TBEM model. Figure 2 shows the amplitude differences in the responses, between the TBEM and MFS solutions, along x , y and z , when $NS = 40$ and $\delta/R = 0.4$.

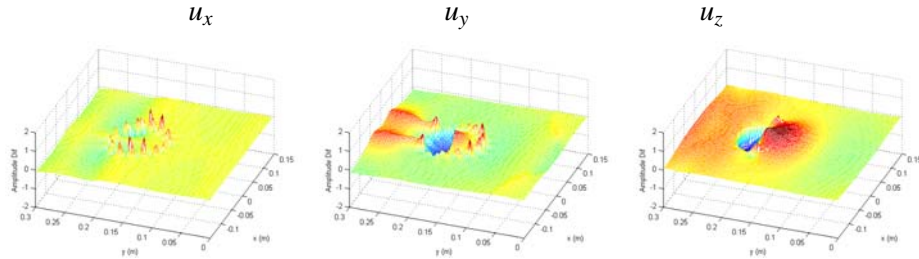


Figure 2: Amplitude differences between the TBEM and MFS solutions.

Analyzing all the computed results, a general trend is observed: the MFS performance is poor, no matter how many virtual sources are used, when they are placed very close to the crack. The minimum errors obtained seem to occur for intermediate values of distances δ/R (0.10 and 0.20).

Numerical Example

The 2D wave propagation near a null-thickness S-shaped crack (see Figure 3), with the properties defined above, is modeled. The domain decomposition technique described above is used with $NS = 600$ and $\delta/R = 0.20$. A dilatational line load ($k_z = 0.0$ rad/m), placed at S, disturbs the elastic layer, where displacements (u_x and u_y) are registered at a grid of receivers. The computations were performed

in the range of [2000 Hz, 256000 Hz]. Time results were determined modeling a Ricker incident pulse with a characteristic frequency of 75000 Hz.

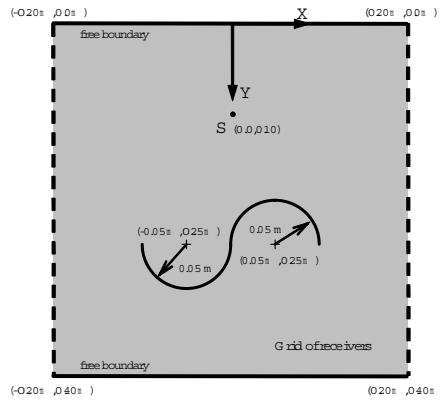


Figure 3: Geometry of S-shaped crack in the elastic slab.

The numerical results obtained are illustrated using snapshots at $t = 0.07$ ms and $t = 0.11$ ms, displaying the displacement fields in the x and y directions (Figure 4). These displacement fields correspond to the direct incident fields produced by the line source added to the surface terms and the scattered fields generated by the irregular crack.

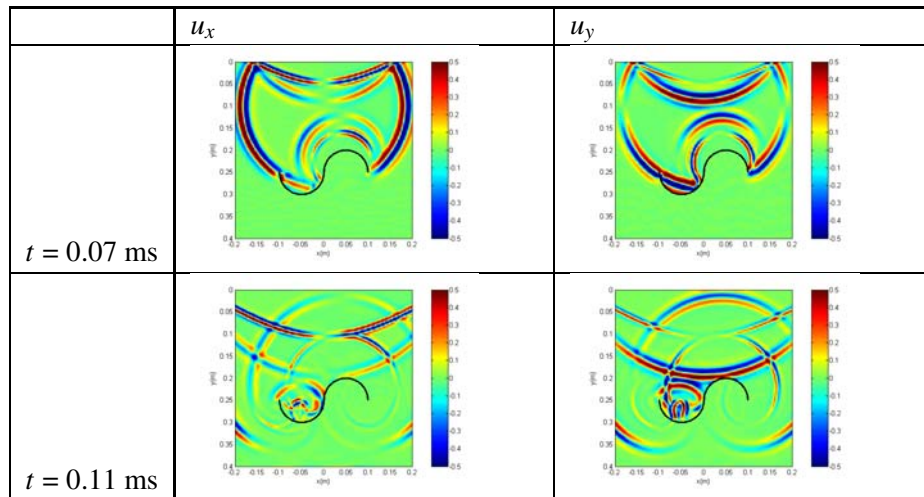


Figure 4: Elastic scattering by an S-shaped crack in an elastic slab.

Conclusions

The TBEM and MFS formulations have been successfully implemented to address the wave propagation in the vicinity of null-thickness empty cracks placed in a slab. The TBEM has been adopted to discretize cracks with an open line

of boundary elements, while the proposed MFS solution has been able to solve the problem without having to use an enriched function to model the displacement jumps across the crack. These formulations were found to produce results that were in close agreement. The MFS was found to be efficient and was able to capture all the elastic wave phenomena involved. However, the definition of the number and placement of the virtual sources to be used needs further research, since this plays an important role in the accuracy of the results.

Acknowledgement

This research work was supported by the Portuguese Foundation for Science and Technology, under the research project POCI/ECM/58940/2004.

References

1. Dell'era, D.N., Aliabadi, M.H. and Rooke, D.P. (1998): "Dual boundary element method for three-dimensional thermoelastic crack problems", *Int. J. Fract.*, Vol. 94, pp. 89-101.
2. Prosper, D. and Kausel, E. (2001): "Wave scattering by cracks in laminated media". In: *Procs. of the ICES'01*, Tech Science Press.
3. Amado Mendes, P. and Tadeu, A. (2006): "Wave propagation in the presence of empty cracks in an elastic medium", *Comput. Mech.*, Vol. 38(3), pp. 183-199.
4. Alves, C.J.S. and Leitão, V.M.A. (2006): "Crack analysis using an enriched MFS domain decomposition technique", *Eng. Anal. Bound. Elem.*, Vol. 30(3), pp. 160-166.
5. Guiggiani, M. (1998): *Formulation and numerical treatment of boundary integral equations with hypersingular kernels. Singular Integrals in Boundary Element Methods*, Computational Mechanics Publications, Southampton (UK) & Boston (USA).
6. Tadeu, A. and António, J. (2002): "Green's Functions for 2.5D Elastodynamic Problems in a Free Solid Layer Formation", *Eng. Struct.*, Vol. 24(4), pp. 491-499.
7. Fairweather, G. and Karageorghis, A. (1998): "The method of fundamental solutions for elliptic boundary value problems", *Adv. Comput. Math.*, Vol. 9, pp. 69-95.